ELSEVIER
Sensors and Actuators A 97–98 (2002) 448–456
SENSORS AND ACTUATORS A PHYSICAL
www.elsevier.com/locate/sna

Fabrication of biomimetic 3-D structured diaphragms

K. Yoo[a,*], C. Gibbons[b], Q.T. Su[b], R.N. Miles[b], N.C. Tien[c]

[a]School of Electrical and Computer Engineering, Cornell University, #117 Phillips Hall, Ithaca, NY 14853, USA
[b]Department of Mechanical Engineering, SUNY, P.O. 6000, Binghamton, NY 13902-6000, USA
[c]Department of Electrical and Computer Engineering, University of California, Davis, CA 95616, USA

Received 4 July 2001; received in revised form 27 November 2001; accepted 4 December 2001

Abstract

We report on a new approach to the fabrication of 3-D structured diaphragms using integrated surface and deep reactive ion etching (DRIE) bulk silicon micromachining on a silicon-on-insulator (SOI) wafer. Polysilicon diaphragms of $1\,\text{mm} \times 2\,\text{mm} \times 1.2\,\mu\text{m}$, and $1\,\text{mm} \times 2\,\text{mm} \times 2.4\,\mu\text{m}$ parylene diaphragms, which are designed for a biomimetic directional microphone and a differential microphone, respectively have been successfully fabricated by our method. The membranes have 20 μm-thick silicon proof masses, solid stiffeners, hollow stiffeners, and 20 μm-deep corrugations to mimic the tympanal membranes of the fly's ears. Acoustic measurements of the diaphragm using laser vibrometry have demonstrated high directional sensitivity of the device. © 2002 Elsevier Science B.V. All rights reserved.

Keywords: 3-D structured diaphragms; Biomimetic devices; Directional sensitivity; Silicon oxide blocks

1. Introduction

Non-planar micromachined diaphragms that make use of corrugations and bosses have become key components in various micromechanical devices such as pressure sensors [1], microvalves [2], micropumps [3], and accelerometers [4]. As new application areas are discovered and specialized devices are designed, more complex diaphragms will be required. However, two well-established methods for fabricating 3-D structured diaphragms have certain drawbacks limiting the design flexibility. In the electrochemical etch-stop technique, which combines anodic passivation of silicon with a reverse bias of *p*–*n* junction, *n*-type silicon is formed either by epitaxial growth or ion implantation and diffusion on a *p*-type wafer. It is impractical to construct a "proof mass" type of 3-D structures on silicon membranes with epitaxially grown *n*-type layers due to the uniform growth of the epi-layer, whereas, it is attainable with ion implanted and diffused *n*-type layer by double diffusion [5]. The second method utilizes heavily boron-doped (p^{++}) layers as etch-stop layers. In most cases, they are ion implanted and diffused. However, these layers can also be epitaxially grown. The stress induced by the high dopant concentration can considerably alter critical mechanical factors such as the resonant frequency of the diaphragm. In addition, the substantial surface damage from implantation precludes the formation of active electronic devices. In both methods, which employ etch-stop layers created by ion implantation and diffusion, the achievable thickness of the structures on diaphragms is upper-bounded by the maximum dopants diffusion depth (on the order of 15 μm) [6].

Our method integrates surface micromachining with bulk silicon micromachining to fabricate 3-D structured membranes [7]. It utilizes the buried oxide layer in a silicon-on-insulator (SOI) wafer as an etch-stop layer. Deep reactive ion etching (DRIE) allows precision patterning of single-crystal silicon (SCS) structures such as proof masses, and stiffeners with aspect ratios higher than 20. The thickness of the structures and the depths of corrugations are determined by the thickness of the device layer on the SOI wafer. Silicon is etched from the backside of the wafer using DRIE, which can achieve deep etching with very high anisotropy (side-wall angles $90 \pm 2^\circ$), unlike conventional methods involving wet anisotropic etchants such as EDP, KOH, and TMAH [6]. Various diaphragm materials such as polysilicon, silicon nitride, and polymers can be selected for different applications, because there is no subsequent thermal processing and no wet chemical backside silicon etching in our method.

To demonstrate the potential of our new approach for the fabrication of 3-D structured diaphragms, we present a biomimetic corrugated polysilicon diaphragm with SCS proof masses and solid stiffeners for a directional microphone, and a corrugated parylene diaphragm with SCS proof

*Corresponding author. Present address: 955 Cranbrook Ct. #207, Davis, CA 95616 USA. Tel.: +1-530-297-5153; fax: +1-509-463-1127.
E-mail address: yoo@ece.cornell.edu (K. Yoo).

0924-4247/02/$ – see front matter © 2002 Elsevier Science B.V. All rights reserved.
PII: S0924-4247(01)00808-1

masses, solid stiffeners, and hollow stiffeners for a differential microphone.

2. Designs

Previous studies on the parasitoid fly *Ormia ochracea* reveal that the fly's ears are mechanically coupled by a flexible bridge, which is utilized to achieve directionality [8]. The mechanical link between ears provides two distinct resonant modes, a rocking mode at the first resonant frequency and an in-phase mode at the second resonant frequency. Linear combinations of these two modes produce distinctive asymmetrical mechanical responses of the tympana, thereby generating mechanical interaural delays and amplitude differences resulting in directionality. Our diaphragm designs (Fig. 1) are based on the mechanical model of the fly's ear [9].

2.1. Diaphragm for a directional microphone

Phosphorous-doped polysilicon is chosen for the diaphragm material for the hearing aids directional microphone. Due to the relatively high Young's modulus of polysilicon (∼170 GPa), the 1 mm × 2 mm × 1.2 μm diaphragm has two 200 μm × 380 μm × 20 μm SCS proof masses on each side to lower the natural frequencies of the diaphragm for the hearing aids application. Also, the diaphragm consists of 5 μm × 960 μm × 20 μm center solid stiffeners and three 10 μm × 970 μm × 20 μm middle solid stiffeners to create the necessary stiffness to achieve the rigid body motion of the two mode shapes. The diaphragm makes use of a corrugation, that is 10 μm-wide and 20 μm-deep to relieve in-plane stress and increase mechanical sensitivity. It is rounded at the corners to reduce stress concentration.

2.2. Diaphragm for a differential microphone

The 1 mm × 2 mm × 2.4 μm diaphragm for a differential microphone is constructed of Parylene C with a Young's modulus of 3.2 GPa. This polymer resembles more closely the tympanal membranes of the fly's ears than polysilicon film in terms of its mechanical properties. Since the differential microphone utilizes only the rocking mode at the first resonant frequency, the diaphragm incorporates hollow skin stiffeners, basically corrugations with various dimensions to

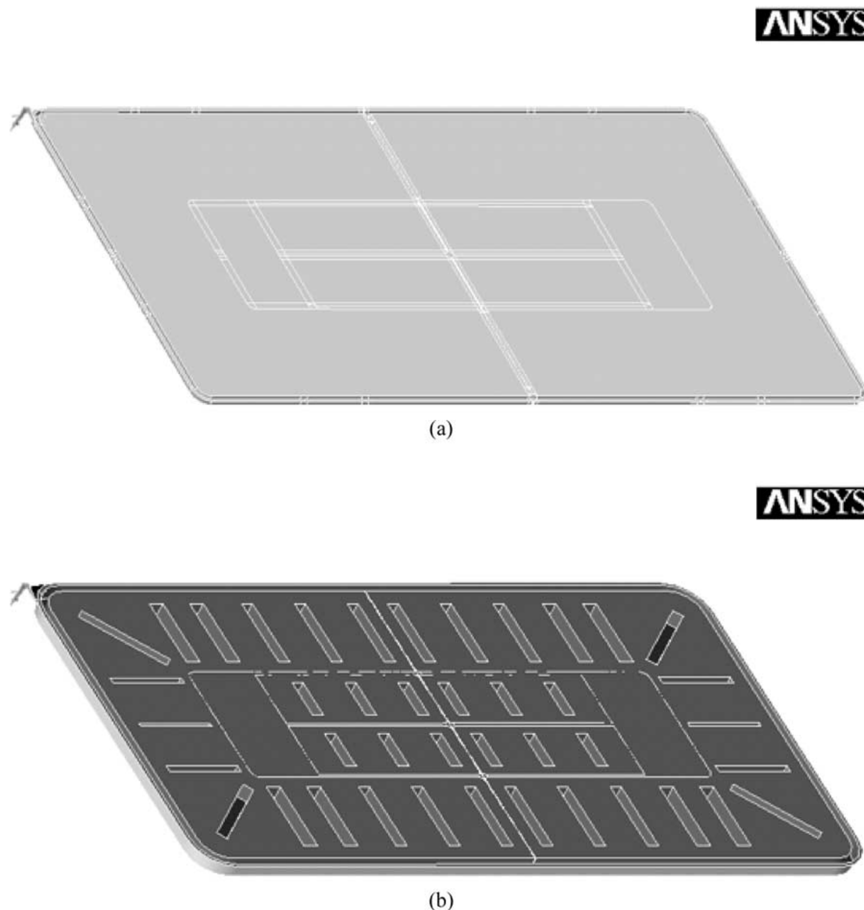

Fig. 1. (a) diaphragm design for a directional microphone, proof masses, solid stiffeners, and a corrugation; (b) diaphragm design for a differential microphone, proof masses, solid stiffeners, hollow stiffeners, and a corrugation.

have all other resonant frequencies as high as possible in the frequency domain. The corrugated diaphragm with local hollow stiffeners benefits from the conformal coating property of parylene. Both the width of corrugation and the radius sweep of the corners of the diaphragm are doubled.

3. Fabrication

Biomimetic diaphragms for directional microphones and differential microphones have been fabricated on 4 in. SOI substrates using integrated surface and DRIE bulk silicon micromachining.

3.1. Oxide block formation

The 3-D structures of the diaphragms are constructed by transforming unwanted bulk silicon into thick silicon oxide blocks and removing them at the releasing step of the process (Fig. 2). These silicon oxide blocks are created by oxidation of closely spaced silicon beams followed by low temperature oxide (LTO) deposition and chemical

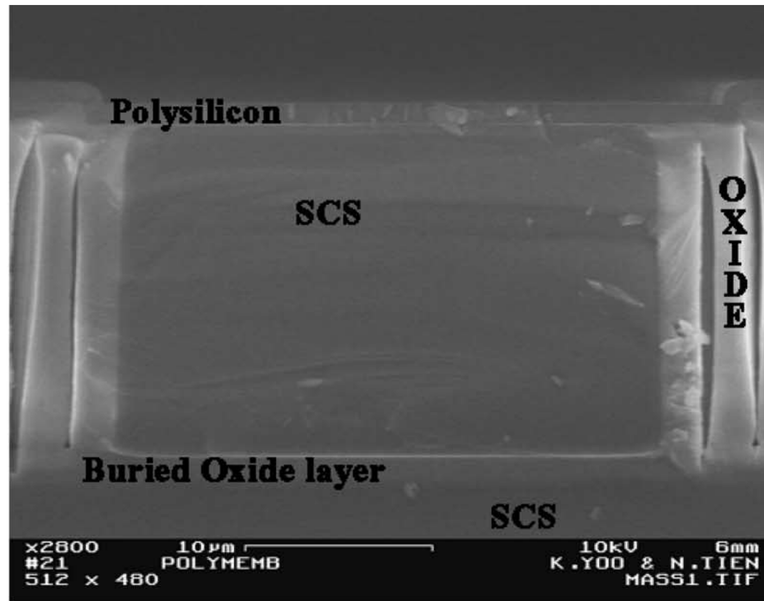

(a)

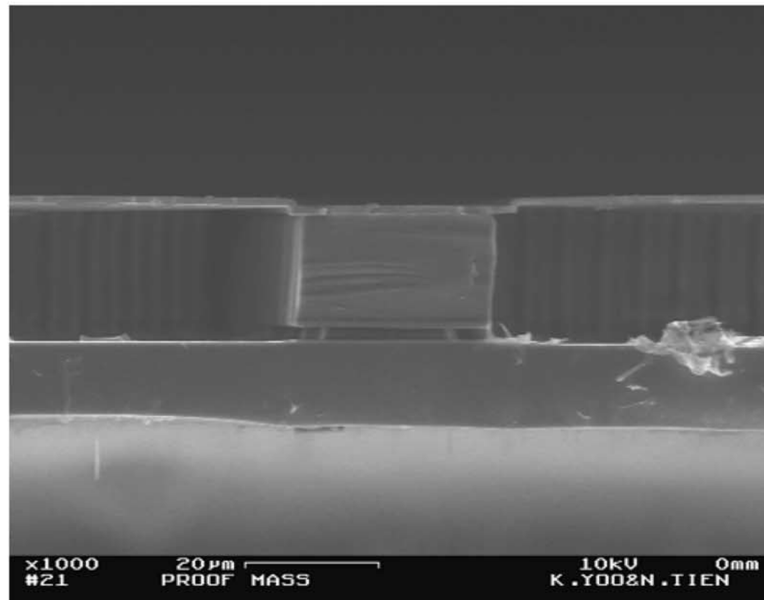

(b)

Fig. 2. SEM image of the cross-sections of a 1.2 μm-thick polysilicon diaphragm with an attached 20 μm-thick SCS proof mass: (a) before release; (b) after release (silicon has not been completely removed by DRIE from the backside of the wafer for obvious reasons of mechanical integrity).

mechanical polishing (CMP). In the earlier works, Yeh et al. [7] and Jiang et al. [10] used 1 μm-wide beams that were 2 μm apart. These lengthy (>100 μm), yet thin beams had 1 μm-wide lateral beams in between to prevent severe lateral bending of the beams due to the volume expansion from oxidation. However, the stress induced by the volume expansion (2.27 times in volume) resulted in the separation gaps between beams as wide as 5 μm, and was relaxed partially by exerting force on the neighboring films and silicon substrate. Firstly, sealing wider trenches requires thicker deposition of oxide, and this oxide layer induces higher stress due to the coefficients of thermal expansion (CTE) mismatch between silicon oxide and the polysilicon diaphragm. This can lead to the cracking of the thin diaphragm prior to the final release in HF. Secondly, incompletely oxidized silicon residues were found at the lower joint corner sections between the beams and the bulk silicon side-walls, and between the beams and the lateral beams. Intuitively, the retardation of oxidation is attributed to the limited supply of oxidants at the lower regions of the beams, but it may also be due to the reduced chemical reaction rate caused by viscous stress [11]. The unoxidized silicon residues attached to the lower bottom of the corrugations can limit the deflection of the diaphragms. In our new silicon

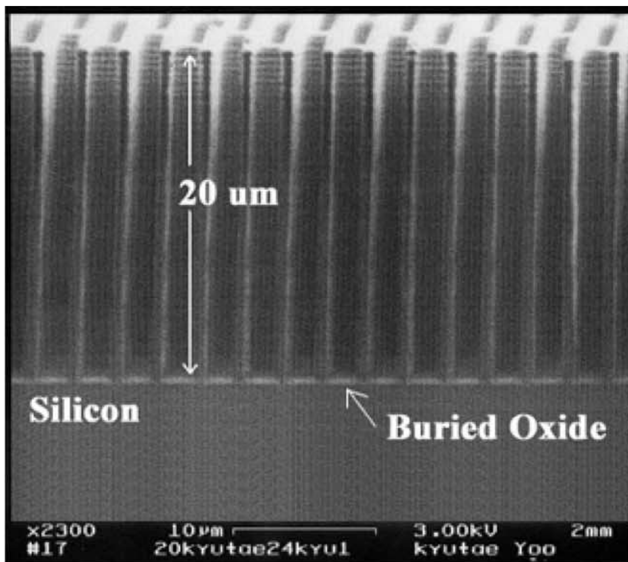

(a)

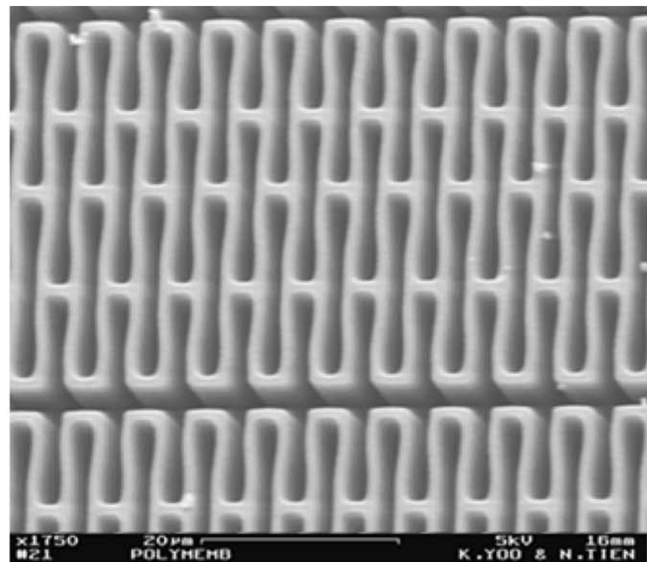

(b)

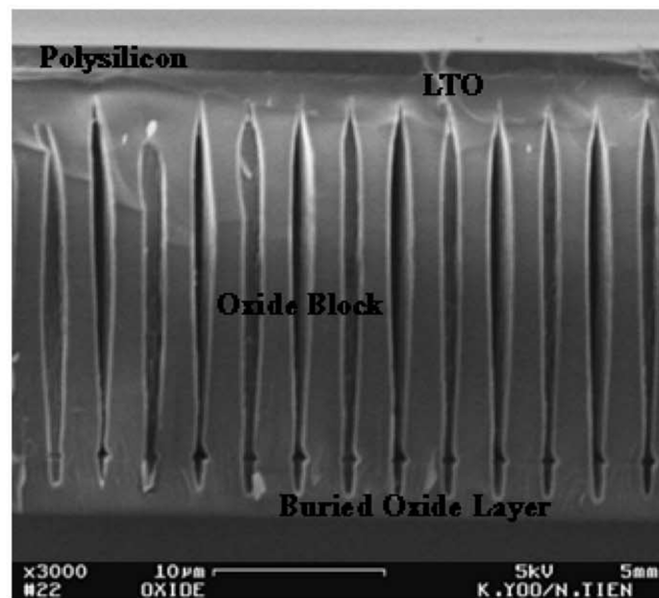

(c)

Fig. 3. (a) Silicon beams in a SOI wafer after DRIE (1 μm-wide, 25–60 μm-long beams that are 2 μm apart); (b) SiO_2 beams after oxidation; (c) SiO_2 block after LTO deposition, followed by CMP.

beam design, the gap widening is minimized by using beams from 25 to 60 μm in length and 1 μm in width, spaced 2 μm apart laterally and vertically to allow for the volume expansion of oxide. Also, thinner 0.8 μm-wide lateral supporting beams are used to enhance the structural rigidity of oxide blocks for the subsequent CMP process. The beams are oxidized in steam at 1150 °C for 200 min to relieve the stress via a viscous flow of oxide. As shown in Fig. 3, there is only a slight bending of the beams and no incompletely oxidized silicon residues left observed after oxidation. The slightly altered gap width (2 ± 0.25 μm) after oxidation between the beams makes it possible to seal the gaps with less LTO.

3.2. Process flow

The process is depicted schematically in Fig. 4. Our starting material is a SOI wafer with 20 μm-thick device silicon and 2 μm-thick buried oxide. The 20 μm-deep trenches are etched using DRIE (Fig. 4a). The silicon beams are thermally oxidized. LTO is deposited at 425 °C to partially fill and completely seal the gaps between the oxidized beams. Once the unwanted silicon is transformed into oxide blocks, the surface is planarized by CMP to allow the subsequent surface micromachining (Fig. 4b). Silicon is etched using DRIE for corrugations and hollow stiffeners (Fig. 4c). For the polysilicon diaphragm, 1.2 μm-thick phosphorus doped polysilicon is deposited at 580 °C and annealed at 1050 °C for 80 min in a dry N_2 ambient to relax compressive residual stress in the film. Rapid thermal annealing (RTA) treatment is also employed followed by the furnace annealing to obtain slightly tensile stress. For the parylene diaphragm, 2.4 μm-thick Parylene C is coated onto the substrate at the room temperature (Fig. 4d). Silicon is removed from the backside of the wafer using DRIE, and the etch-stops at the buried oxide layer (Fig. 4e). Using a hydrofluoric acid solution, the oxide blocks are removed, and the corrugated diaphragms with proof masses are released (Fig. 4f). Figs. 5 and 6 show the fabricated polysilicon and parylene diaphragms.

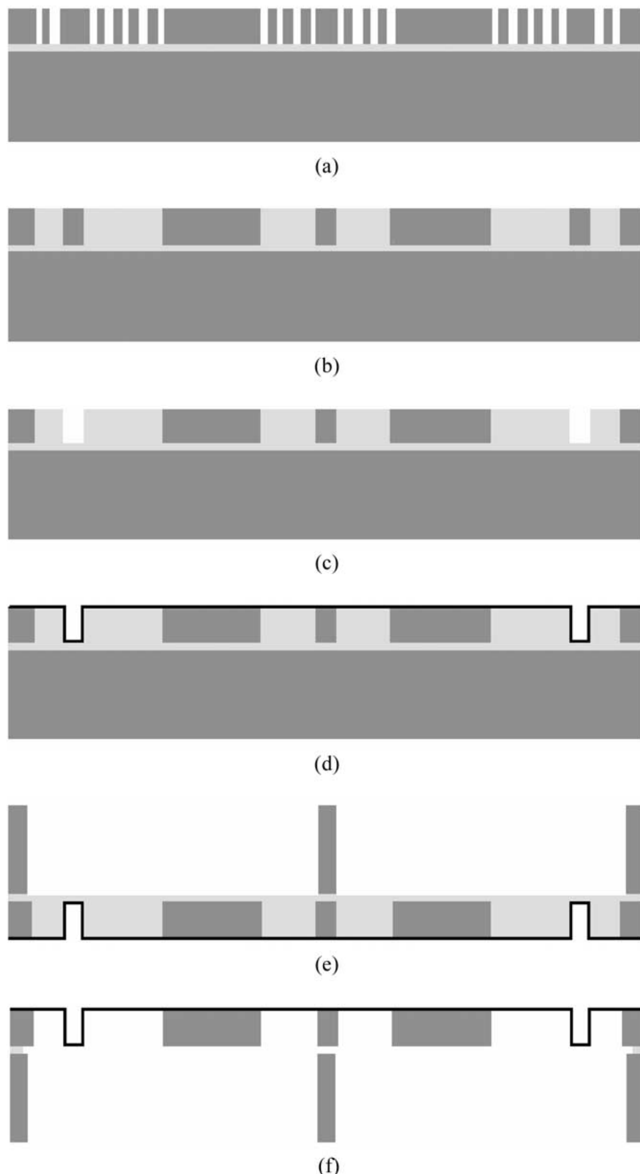

Fig. 4. Fabrication process flow.

4. Results

The polysilicon diaphragm for a directional microphone, and the parylene diaphragm for a differential microphone have been tested by the laser vibrometry method to acquire measurements of the sound induced vibrations of the diaphragm. The testing set-up consists of a Polytec laser vibrometer (OFV 302 optical-head and OFV-2100 electronics unit), a loudspeaker, and a reference microphone (B&K 4138). The displacements at 25 locations on the diaphragm were measured as a function of frequency. The incident sound waves are generated by a loudspeaker positioned at 45° angle relative to the longitudinal axis of the diaphragm.

Fig. 7a and b show the transfer functions between the displacements of the diaphragms and the incident sound pressure with a reference level of 1 mm/Pa for the polysilicon and parylene diaphragms, respectively. In Fig. 7a, the point closer to the sound source (point A) responds with greater amplitude than the point further from the source (point B) over a wide frequency range. The response at the pivot point c is much smaller than those at other two locations by 20 dB or greater. The sharp peak of the transfer functions at 8 kHz is due to the resonant frequency of the sample holder, not the diaphragm. The parylene diaphragm shows the similar frequency responses within the limited frequency range from 32 kHz to 38 kHz (Fig. 7b), however, the difference in amplitudes is much smaller compared to that of polysilicon diaphragm.

In Fig. 8, the deflection shapes of the polysilicon diaphragm for three different frequencies are shown. At the first resonant frequency (∼16 kHz), the diaphragm rocks about the pivot point (Fig. 8a). On the other hand, at the second

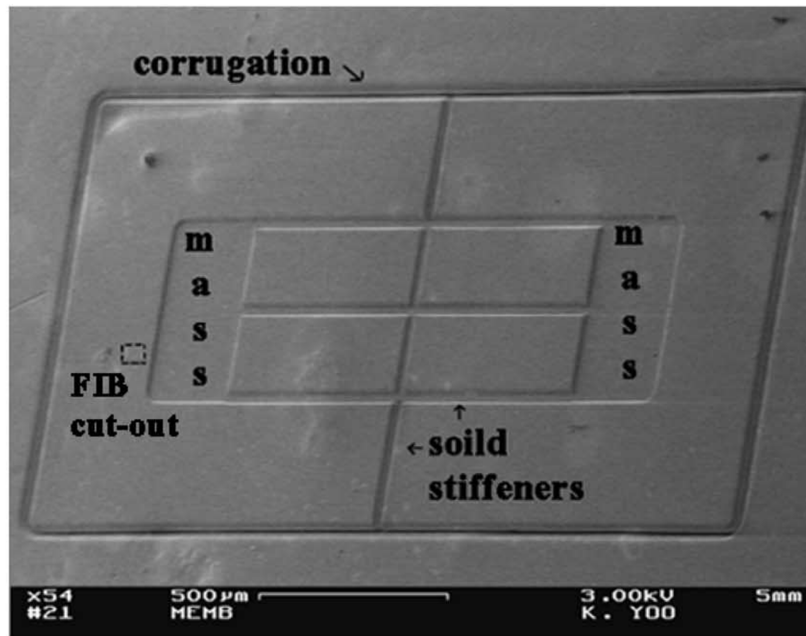

(a)

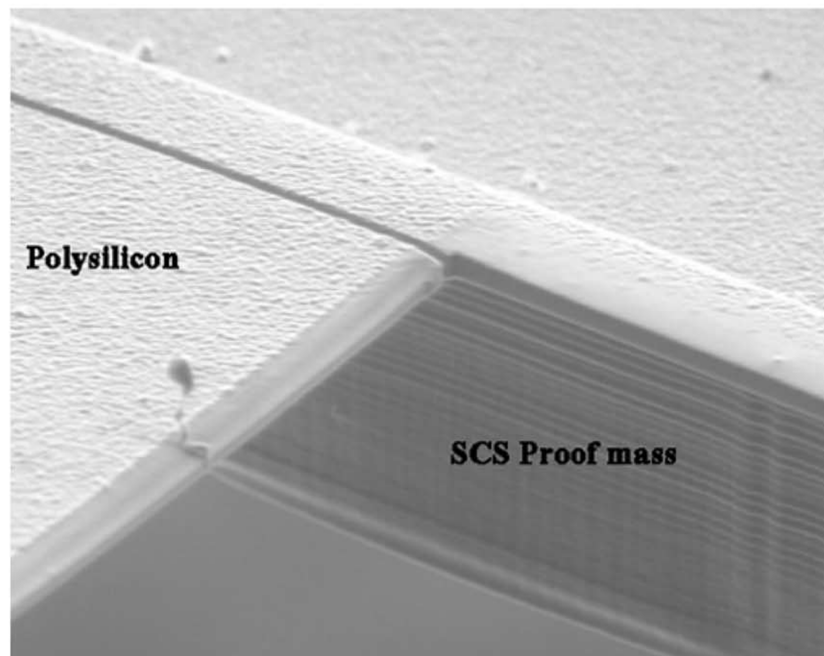

(b)

Fig. 5. SEM images of diaphragms: (a) the polysilicon diaphragm; (b) a close-up image of a SCS proof mass attached to the polysilicon diaphragm through the window cut by focused ion beam (FIB).

resonant frequency (∼25 kHz), both sides of the diaphragm move with the same amplitude and phase (Fig. 8b). Frequencies between the first and second resonant frequencies result in the linear combination of these two modes producing asymmetric shapes of the diaphragm with a significant difference in amplitude, thus providing directionality (Fig. 8c). The results demonstrate that the polysilicon diaphragm has very similar mode shapes when responding to sound pressure and directional sensitivity compared to the fly's ears. The parylene diaphragm also exhibits the rocking mode at the first resonant frequency (∼33 kHz), and the translational mode at the second resonant frequency (∼38 kHz), however, these frequencies are much higher than predicted values by finite element method (FEM). The primary cause for this discrepancy is the fact that the tensile stress of the film due to the considerable mismatch in CTEs between the palylene film and the substrate has increased the resonant frequencies by the square root of the film's stress.

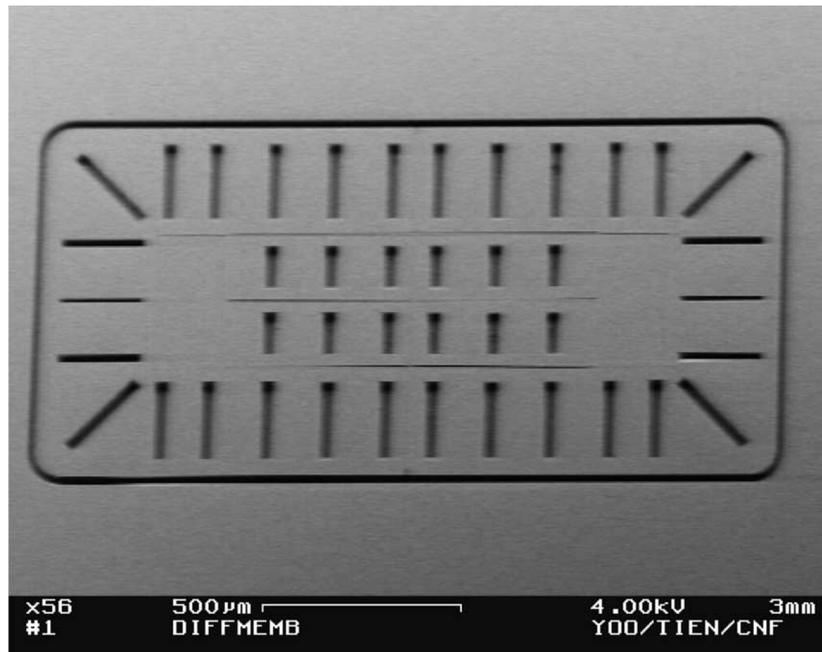

Fig. 6. SEM image of the aluminum coated parylene diaphragm.

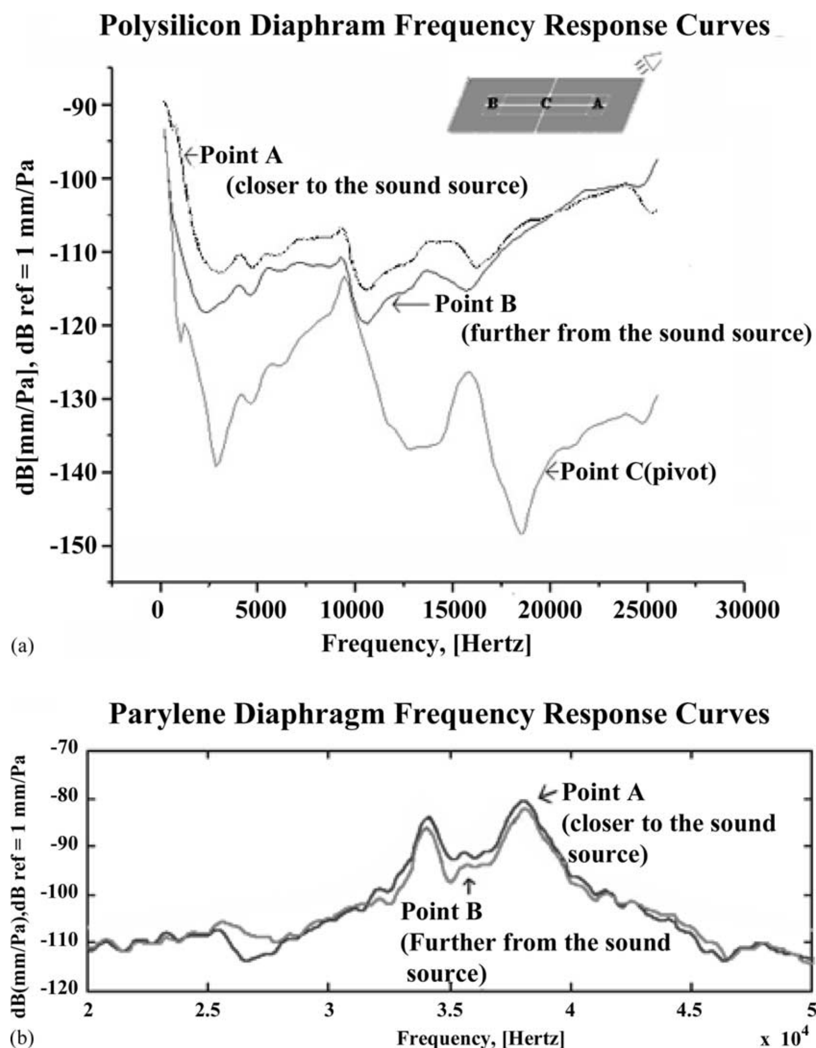

Fig. 7. (a) Measured frequency response curves of the polysilicon diaphragm; (b) measured frequency response curves of the parylene diaphragm.

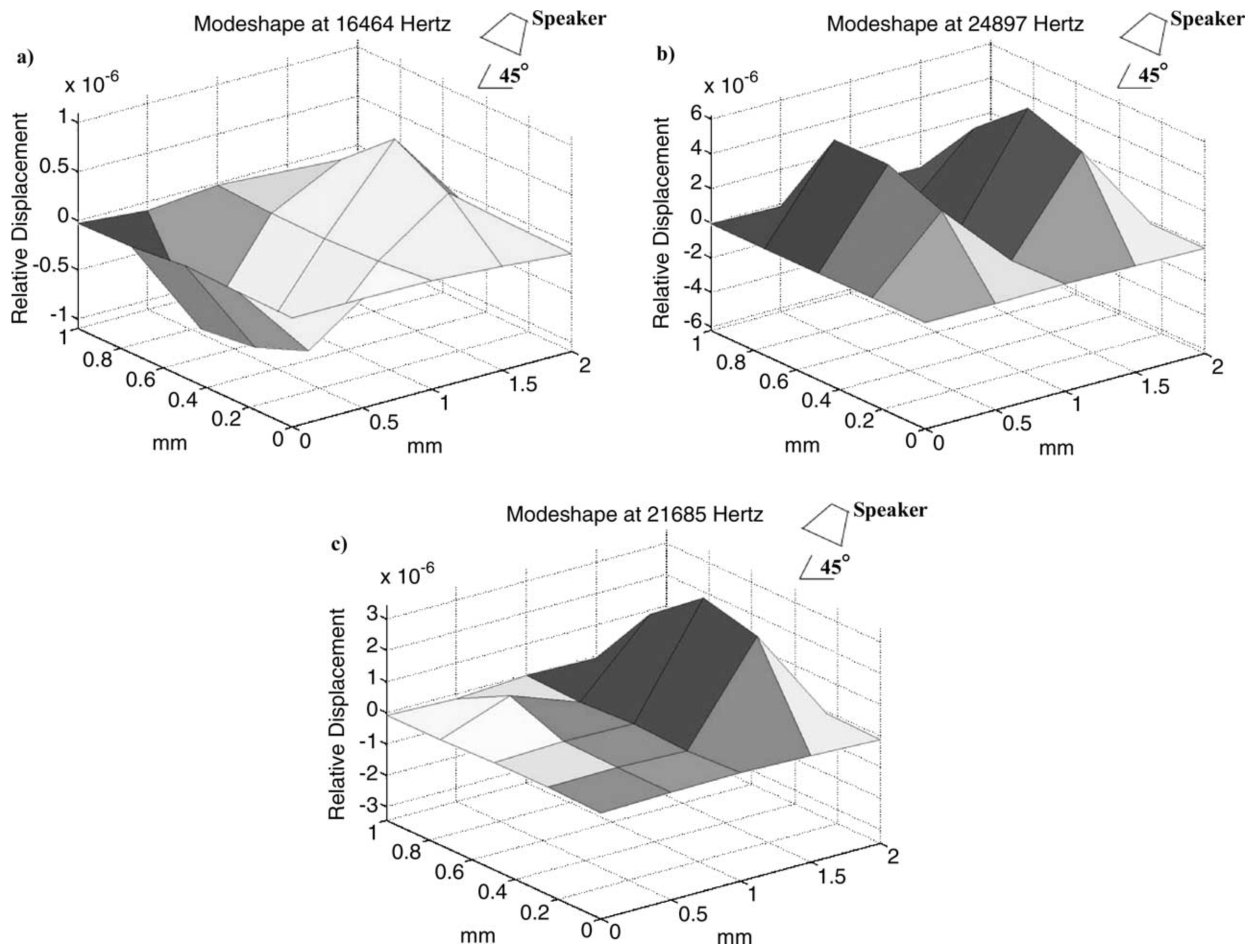

Fig. 8. Measured displacements at 25 different locations on the polysilicon diaphragm: (a) a rocking mode shape at the first resonant frequency; (b) an in-phase mode shape at the second resonant frequency; (c) an asymmetric mode shape at a random frequency between the first and second resonant frequencies.

5. Conclusion

The novel approach to the fabrication of non-planar diaphragms using integrated surface and DRIE bulk silicon micromachining on a SOI wafer offers vital advantages of excellent precision in dimensions of the structures, and high flexibility in designs over conventional etch-stop techniques. A range of materials including polysilicon, silicon nitride, and polymer can be selected for the diaphragm depending on the applications. Our method makes use of DRIE, which can produce very high aspect ratio holes with perpendicular side-wall angles ($90 \pm 2^{\circ}$) to etch silicon from the backside of the wafer. This enables us to build arrays of closely spaced diaphragms for various MEMS applications such as ultra-sound imaging transducers. Furthermore, the variations in the dimensions of the diaphragms due to the thickness variations of the wafer itself can be minimized. Our method has been applied to polysilicon and parylene diaphragms for a directional microphone and a differential microphone, respectively. These diaphragms incorporate corrugations, proof masses, and stiffeners to mimic the ears of the para-sitoid fly, *Ormia ochracea.* The successfully fabricated diaphragms exhibit two resonant modes of vibration, and the linear combination of these two modes provide the directional sensitivity required in a directional microphone hearing aids system.

Acknowledgements

The author would like to thank Steven Herschbein, and Aron Shore of IBM for FIB service, Dr. Pai and Dr. Tsai of Rockwell Science Center for parylene coating and the staff of the Cornell Nanofabrication Facility. The authors also would like to thank D.T. McCormick, K.V. Madanagopal, Dr. Li, Y. Wang, H. Jiang, S. Kommera, H.T. Kim and C.C. Liu for useful discussions.

References

[1] L. Christel, K. Petersen, P. Barth, F. Pourahmadi, J Mallon .Jr., J. Bryzek, Single-crystal silicon pressure sensors with 500× over-pressure protection, Sens. Actuators A21–23 (1990) 84–88.

[2] J. Franz, H. Baumann, H-P. Trah, A silicon microvalve with integrated flow sensor, Technical Digest, in: Proceeding of the 8th International Conference Solid-State Sensors and Actuators (Transducers'95), Stockholm, Sweden, 25–29 June 1995, p. 313.
[3] J. Zou, X.Y. Ye, Z.Y. Zhou, Y. Yang, A novel thermally-actuated micropump, in: Proceedings of the International Symposium on Micromechatronics and Human Science, Nagoya, Japan, 1997, 231–234.
[4] D. Lapadatu, A. Pyka, J. Dziuban, R. Puers, Corrugated silicon nitride membranes as suspensions in micromachined silicon accelerometers, J. Micromech. Microeng. 6 (1996) 73–76.
[5] S. Marco, J. Samitier, J. Morante, A. Gotz, J. Esteve, Three-dimensional structures obtained by double diffusion and electrochemical etch-stop, J. Micromech. Microeng. 3 (1993) 141–142.
[6] G.T.A. Kovacs. Micromachined Transducers Sourcebook, McGraw-Hill, New York, 1998.
[7] J.-L.A. Yeh, H. Jiang, N.C. Tien, Integrated polysilicon and DRIE bulk silicon micromachining for an electrostatic torsional actuator, J. Microelectromech. Syst. 8 (4) (1999) 456–465.
[8] R.N. Miles, D. Robert, R.R. Hoy, Mechanically coupled ears for directional hearing in the parasitoid fly *Ormia ochracea*, J. Acoust. Soc. Am. 98 (6) (1995) 3059–3070.
[9] C. Gibbons, Design of a biomimetic directional microphone diaphragm, Masters Thesis, Binghamton University, 2000.
[10] H. Jiang, Y. Wang, J.-L.A. Yeh, N.C. Tien, Fabrication of high-performance on-chip suspended spiral inductors by micromachining and electroless copper plating, in: Proceedings of the Dig. IEEE MTT-S International Microwave Symposium, Boston, USA, 2000, 279–282.
[11] D-B. Kao, J.P. Mcvittie, W.D. Nix, K.C. Saraswat, Two-dimensional thermal oxidation of silicon-II. Modeling stress effects in wet oxides, IEEE Trans. Electron. Devices 35 (1988) 25–37.

Biographies

Kyutae Yoo received the BS and MS degrees from Cornell University, Ithaca, NY, in 1997 and 2001, respectively, where he is currently working toward the PhD degree all in electrical engineering. His research interests are in acoustic MEMS sensors, biomimetic MEMS devices, and micromachined ultrasonic transducers (MUTs).

Colum Gibbons received his BS and MS in Mechanical Engineering from Binghamton University in 1998 and 2000, respectively. His research background covered finite element analysis, vibrations and MEMS devices. All three were used in his graduate studies as he worked to codesign a biomimetic acoustic MEMS diaphragm along with Dr. Ronald N. Miles of Binghamton University. He is currently working in the FEA field at Analysis and Design Application Corporation Ltd. in Melville, New York.

Quang Su received the BS degree in mechanical engineering from the State University of New York at Binghamton in 1998. He is currently working towards his PhD degree in mechanical engineering there under the advisory of Dr. Ronald N. Miles. Current research interests include acoustic response measurement and prediction using laser vibrometry, spectral analysis, and parametric methods.

R.N. Miles received a BSEE from UC Berkeley in 1976, a MSE in 1985, and a PhD in 1987, both from the University of Washington. Beginning in 1977 he worked in the acoustics staff at Boeing for 8 years. He was an assistant research engineer and lecturer in the Department of Mechanical Engineering at UC Berkeley from 1/1987 to 12/1988. He has been with the Department of Mechanical Engineering at the State University of New York at Binghamton since 1989 where he is now Professor and Chairman.

Norman C. Tien is an associate professor in the Department of Electrical and Computer Engineering at the University of California at Davis and a Co-Director of the Berkeley Sensor and Actuator Center (BSAC). Prior to joining U.C. Davis in 2001, Tien was an associate professor in the School of Electrical and Computer Engineering at Cornell University. From 1993 to 1996, he was a lecturer in the Department of Electrical Engineering and Computer Science at the University of California, Berkeley and a postdoctoral research engineer at the BSAC. Between 1984 and 1986, he was a silicon process development engineer at the Microelectronics Center of Polaroid Corporation, in Cambridge, MA. Dr. Tien received a BS degree from the University of California, Berkeley, a MS degree from the University of Illinois, Urbana-Champaign, and a PhD from the University of California, San Diego.